DFT insight into the high stability of single Pt atoms on the CeO$_2$(111) surface

Ho Viet Thang[1,*], Van Quy Hop[1], Thong Le Minh Pham[2,3]

Use your smartphone to scan this QR code and download this article

[1]*The University of Danang, University of Science and Technology, 54 Nguyen Luong Bang, Da Nang City 550000, Vietnam.*

[2]*Institute of Research and Development, Duy Tan University, Da Nang City 550000, Vietnam*

[3]*Faculty of Environmental and Chemical Engineering, Duy Tan University, Da Nang, 550000, Vietnam*

Correspondence

Ho Viet Thang, The University of Danang, University of Science and Technology, 54 Nguyen Luong Bang, Da Nang City 550000, Vietnam.

Email: hvthang@dut.udn.vn

VNUHCM PRESS
25 years of scholarly publishing
1997-2022

ABSTRACT

Introduction: Single Pt atom catalysts supported on CeO$_2$(111) surfaces have attracted considerable attention in recent years due to their high reactivity and selectivity in important reactions, such as water–gas shift reactions for hydrogen production and CO oxidation. However, the geometrical and electronic structure of Pt/CeO$_2$(111) at the atomic level is still not clearly understood. In this study, we aim to gain insight into the geometrical and electronic structure of a single Pt atom on the CeO$_2$(111) surface. **Methodology:** Various single Pt atom species, including (Pt)$_{ads}$, (PtOH)$_{ads}$, (PtO)$_{ads}$, (PtO$_2$H$_2$)$_{ads}$, (PtO$_2$)$_{ads}$, (Pt)$_{subCe}$, and (Pt)$_{subO}$, deposited on the CeO$_2$(111) surface were investigated by the DFT+U method with dispersion corrections. Furthermore, the CO molecule was adopted to evaluate the electronic structures of these single Pt atoms. In addition, the supported Pt$_3$ cluster was applied as a metallic model to distinguish it from single Pt atom models. **Results:** By comparing the CO adsorption properties of single Pt atom models and Pt$_3$ cluster models to those of experimental observations in the literature, the stretching frequency of CO on (PtO$_2$)$_{ads}$ species agrees well with the experimental results, while the frequencies of CO on other single Pt atom structures and on Pt$_3$ clusters largely differ from the experimental results. **Conclusion:** Based on the DFT calculated results, we conclude that the activity and high stability of single Pt atom species that were observed from the experiment are formed via the interaction between Pt and two extra O atoms on the CeO$_2$(111) surface.

Key words: single atom catalyst, Pt, CeO$_2$(111), Pt/CeO$_2$(111), CO adsorption, DFT+U

INTRODUCTION

Heterocatalysts consisting of precious metals deposited on metal oxide surfaces have attracted considerable attention for environmental remediation, such as CO$_2$ conversion and CO oxidation.[1–4] Depending on the synthesis and catalytic processes, different sizes of precious metals were deposited on the metal oxide support. However, in many cases, precious metals cannot be used efficiently (i.e., 100%), and the selectivity is difficult to evaluate. Therefore, reducing the size of precious metals to obtain the maximum efficiency and high selectivity in catalytic processes is essential. This boosts the scientific communities in the world and has spent much effort on this field in recent years aiming at reducing the size of precious metals as little as possible. As a result, the size of supported precious metals was reduced from nanoparticles to cluster species, and the ultimate size was atomic species.[5] The pioneering work has obtained the atomic size of precious metal Pt dispersed on FeO$_x$ materials[6], and it has shown an excellent catalytic activity and high selectivity for CO oxidation compared to Pt clusters or Pt nanoparticles. This paves the way for numerous studies of different single metal catalysts supported

on different supporting materials, including metal oxides, metals, MOFs, graphene, and zeolites.[7] However, the high surface energy of these single atom species gives rise to the aggregation forming particles. To avoid this obstacle, many techniques have been proposed and successfully synthesized, such as creating void space, chelating, functional groups, etc.[8] Among metal catalysts, Pt supported on CeO$_2$ materials has been widely used in the control of vehicle exhaust.[9] Owing to its high thermal stability, catalytic activity and selectivity. Furthermore, the atomic dispersion of Pt on CeO$_2$ has been experimentally synthesized and demonstrated the efficient utilization of Pt atom catalysts.[10–12] However, the electronic nature of a single Pt atom deposited on CeO$_2$, such as the local structure, chemical state and dynamics during catalytic processes, is still not clearly understood even with state-of-the-art experimental methods. To shed light on the high stability and catalytic activity of a single Pt atom on the CeO$_2$ supporting material, we systematically investigated the atomic dispersion of Pt species on the most stable CeO$_2$(111) surface by applying the DFT+U approach with dispersion correction. The geometrical and electronic properties of

various single Pt atom configurations were evaluated and probed by the adsorption energy and stretching frequencies of CO.

COMPUTATIONAL METHODS AND MODELS

Spin-polarized density functional theory (DFT) calculations were carried out by using the Vienna ab initio simulation package (VASP 5.4.1).[13] The generalized gradient approximation (GGA) with the Perdew-Burke-Ernzerhof (PBE) functional[14] was adopted to evaluate the electron exchange-correlation. The core electrons and nuclei interactions were described by the projector augmented wave (PAW)[15], while the valence electrons of atoms explicitly considered are Ce (5s, 5p, 6s, 4f, 5d), Pt (6s, 5d), H (1s), O (2s, 2p) and C (2s, 2p). To partly compensate for the lack of self-interaction in the DFT method, we applied DFT+U as suggested by Dudarev et al.(16) In this work, Hubbard's parameter U[16,17] of 4.5 eV was applied for the Ce 4f state[18], and with this U parameter, we reproduced the cell parameters (a=b=c=5.472 Å) in good agreement with that of the experiment (a=b=c=5.411 Å).[19] Furthermore, the dispersion correction was also included by using the D3 scheme of Grimme.[20] All calculations were considered at the G point only with a plane wave basis set within a cutoff energy of 400 eV.[21] The geometrical structure optimization was obtained when the ionic forces were less than 0.01 eV/Å. The nine-atomic layer slab of the (2x2) supercell corresponding to the stoichiometric formula of $Ce_{48}O_{96}$ was modeled for the most stable $CeO_2(111)$ surface.[22] A vacuum thickness of 15 Å was included in the slab to minimize the interaction between the neighboring slabs. The structural model is shown in Figure 1. Compared to O and Ce in the bulk materials, where the coordinate numbers of O and Ce are 4 and 8, respectively, the coordinate numbers of surface O and Ce are 3 and 7, respectively.

The binding energies (BE in eV) of the single Pt atoms on the $CeO_2(111)$ surface were computed using the following formula:

BE = E(Pt) + E (suf) – E(Pt/surf)[23]

where E(Pt), E(surf) and E(Pt/surf) are the total energies of the isolated Pt atoms, $CeO_2(111)$ surface and combined $Pt/CeO2(111)$ surface, respectively.

The CO adsorption energies, E_{ads} (in eV), were computed as follows:

E_{ads} = E(catal) - E(CO) - E(CO_catal)[12,24,25]

where E(catal), E(CO), and E(CO_catal) are the total energies of single Pt atom species on $CeO_2(111)$ or $CeO_2(111)$ surfaces, of CO molecules and of CO

adsorption complexes on single Pt atom species on $CeO_2(111)$ or $CeO_2(111)$ surfaces, respectively. According to this calculation, the positive values imply stable CO adsorption. The stretching frequencies of adsorbed CO molecules were evaluated within the harmonic approximation, in which CO and its nearest neighboring atoms were taken into account in this calculation. The CO bond length of 1.144 Å and stretching frequency of 2125 cm^{-1} are obtained for the free CO molecule by PBE functional theory. For comparison with the stretching frequencies of those in the experiments, a scaling factor a = 2143/2125 = 1.0085 was used for all theoretical frequencies,[24,26] in which the experimental frequency of the free CO molecule was 2143 cm^{-1}.[27] The effective atomic charge was calculated using the Bader method, which was developed by Henkelman et al.[28]

RESULTS

Single Pt atom species on $CeO_2(111)$ surface

To investigate the nature of the stability of a single Pt atom deposited on the $CeO_2(111)$ surface,[10,11,29] all possible models of single Pt atom species were considered, including adsorbed Pt atom $(Pt)_{ads}$, $(PtOH)_{ads}$,$(PtO_2)_{ads}$, $(PtO_2H_2)_{ads}$, Pt substitutional to Ce site $((Pt)_{subCe})$ and Pt substitutional to O site $((Pt)_{subO})$. These models have been proposed based on the experimental results by state-of-the-art equipment.[24,30] To evaluate the chemical state of a single Pt atom species, we define the formal charge of a single Pt atom model based on its chelation with extra O atoms. In particular, 0 for adatom $(Pt)_{ads}$, I for $(PtOH)_{ads}$ and $(PtO)_{ads}$ species, II for $(PtO_2H_2)_{ads}$ and $(PtO_2)_{ads}$ species; for Pt substitutional to Ce and O sites, the formal charge of Pt is the same as these cations and anions, i.e., +IV and –II for $(Pt)_{subCe}$ and $(Pt)_{subO}$, respectively. The characteristics of these single Pt atom species are described as follows.

An adsorbed Pt atom, $(Pt)_{ads,}$ can stabilize on different sites on the $CeO_2(111)$ surface, consisting of hollow, top O and top Ce sites (Figure 1). We considered these sites and showed that the most stable site is the hollow site. However, Pt does not reside at the center of the hollow site it spontaneously moves and is strongly bound to two O surface atoms with a binding energy of 3.17 eV and with a Pt-O bond length of 3.278 Å (Figure 2a). The Bader charge of $(Pt)_{ads}$ is 0.04 |e|, indicating the neutral charge of Pt. This is consistent with our designation of a formal charge of 0 for the $(Pt)_{ads}$ structure.

The single Pt atom can reside on $CeO_2(111)$ as a $(PtOH)_{ads}$ structure if Pt interacts with one OH group

on the CeO_2(111) surface. In this configuration, Pt is bound to two O atoms from the CeO_2(111) surface with distances of 2.058 and 2.283 Å and bound to one extra O (of OH group) with a distance of 2.039 Å (Table 1 and Figure 2b). We can see that the Pt bound is much stronger on the CeO_2(111) surface as a Pt(OH)$_{ads}$ structure with a binding energy of 5.23 eV, as evidenced by the reduced Pt-O bond length compared to the (Pt)$_{ads}$ structure and the higher oxidation state of Pt due to charge transfer from Pt to CeO_2(111), which is confirmed by the Bader charge of Pt of 0.38 |e| (Table 1). The interaction between Pt and OH groups can give rise to a condensation process, resulting in the formation of (PtO)$_{ads}$ species and 1/2 H_2 in the gas phase. In (PtO)$_{ads}$ species, Pt is also strongly bound to the CeO_2(111) surface and has extra O with an adsorption energy of 6.00 eV. Similar to the (PtOH)$_{ads}$ species, Pt is bound to two surface lattice O atoms with bond lengths of 2.022 and 2.324 Å and bound to one extra O atom with a bond length of 1.887 Å (Table 1 and Figure 2c). However, a larger charge was observed for Pt in (PtO)$_{ads}$ with a Bader charge of 0.57 |e| compared to (PtOH)$_{ads}$ species (0.38 |e|), Table 1. This indicates that the oxidation state of Pt is I in good agreement with previous studies of Pt on TiO_2.[24,26]

The Pt atom can anchor on the CeO_2(111) surface by interacting with two OH groups, forming the (PtO$_2$H$_2$)$_{ads}$ structure. In this configuration, Pt is bound to 4 atoms, two from surface lattice atoms with a distance of 2.024 Å and two extra O atoms with a distance of 2.063 Å (Table 1 and Figure 2d). The increasing number of coordinates of Pt with O atoms results in an increasing charge of Pt, illustrated by the Bader charge of 0.75 |e|, which was designed as the oxidation state of II (Table 1). In this structure, Pt is very strongly bound to the CeO_2(111) surface with a binding energy of 7.95 eV (Table 1). Similar to the case of (PtO)$_{ads}$, Pt interacts with two OH groups that can induce (PtO$_2$)$_{ads}$ and H_2 molecules, resulting from the condensation process. In the (PtO$_2$)$_{ads}$ structure, Pt is also strongly bound to the extra O atoms with a binding energy of 8.82 eV, indicated by reducing the Pt-O distance to 1.843 and 1.856 Å compared to those in the (PtO$_2$H$_2$)$_{ads}$ structure (2.063 Å) and increasing the bond length between Pt and lattice O with distances of 2.101 and 2.169 Å, Table 1 and Figure 2e.

Furthermore, a single Pt atom can exist at either the Ce or O vacant site. These defect sites were formed during the synthetic or catalytic process.[31] Therefore, we also considered these configurations. At the Ce vacancy or Pt substitutional to the Ce site, (Pt)$_{subCe}$, Pt bound to six lattice O atoms with Pt-O bond lengths

from 2.098 to 2.175 Å (Table 1 and Figure 2f). Among single Pt atom species, Pt bound to the largest number of O atoms, resulting in the largest Bader charge of 1.35 |e| and the largest binding energy of 10.60 eV (Table 1).
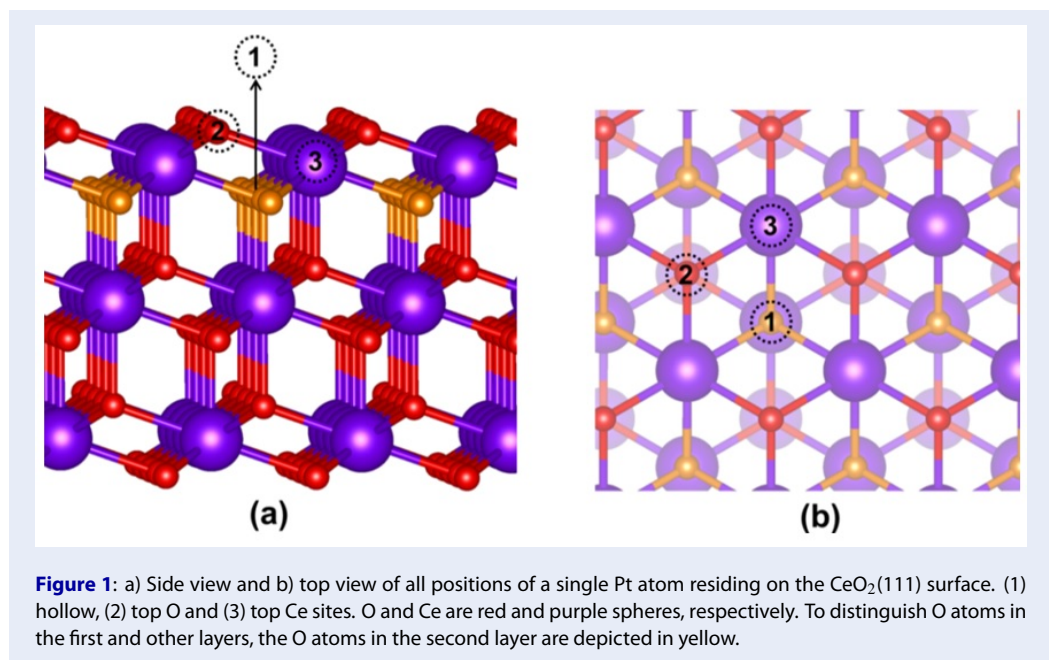
The last configuration is Pt substitutional to lattice O atoms, (Pt)$_{subO}$. At this site, the Pt atom moves up to the surface, resulting in a large distance between Pt and O of 3.290 Å (Figure 2g). In contrast to other single Pt atom structures, Pt accepts the charge from O vacancies, as evidenced by the negative Bader charge of -0.86 |e|, Table 1. At this site, Pt is bound to the CeO_2(111) surface with a binding energy of 4.11 eV.

CO adsorption properties on supported single Pt atom structures

To evaluate the electronic properties of single Pt atom species deposited on the CeO_2(111) surface, CO was used as a probe molecule because CO is sensitive to changes in the electronic structure of materials.[32] Moreover, the CO molecule has been experimentally applied in many oxidation processes based on these catalysts.

First, we considered the CO adsorption properties on the pristine CeO_2(111) surface, in which CO physisorbed on the Ce(IV) site with an adsorption energy of 0.31 eV. The weak adsorption of CO on pristine material is illustrated by a large distance of 2.82 Å between CO and Ce(IV), Table 1 and Figure 3a. The CO bound to the Ce(IV) site is mainly controlled by the electrostatic interaction generated by the local electronic field of the Ce(IV) cation and CO molecule.[33] This gives rise to a reduction in the CO bond length to 1.142 Å compared to CO in the gas phase (1.144 Å) at this theoretical level. As a consequence, the stretching frequency of CO is redshifted by 25 cm^{-1} with respect to the free CO molecule.

Different from the pristine CeO_2(111) surface, a strong adsorption of CO was found when CO was placed on (Pt)$_{ads}$ species with an energy of 3.52 eV. The strong interaction between CO and Pt atoms is due to the effect of "π-back donation" from the 4d electrons of Pt to the antibonding $2\pi^*$ orbital of the CO molecule.[34] As a result, the CO bond length is prolonged to 1.169 Å compared to free CO (1.144 Å), resulting in a large redshift (-96 cm^{-1}) in the stretching frequency of CO (2047 cm^{-1}) with respect to free CO (2143 cm^{-1}) (Table 2). Furthermore, the strong adsorption of CO on (Pt)$_{ads}$ species was demonstrated by a shortened C-Pt distance (1.812 Å) compared to C-Ce(IV) (2.820 Å), Table 2 and Figure 3b.

Figure 1: a) Side view and b) top view of all positions of a single Pt atom residing on the CeO$_2$(111) surface. (1) hollow, (2) top O and (3) top Ce sites. O and Ce are red and purple spheres, respectively. To distinguish O atoms in the first and other layers, the O atoms in the second layer are depicted in yellow.

Table 1: Bond length between Pt and O, r(Pt-O), Bader charge, Q(Pt) and binding energies, BE of single atom Pt species deposited on CeO$_2$(111) surface.

System	r(Pt-O) (Å)	Q(Pt) (|e|)	BE (eV)
(Pt)$_{ads}$	3.278	0.04	3.17
(PtOH)$_{ads}$	2.039; 2.060; 2.283	0.38	5.23
(PtO)$_{ads}$	1.887; 2.022; 2.324	0.57	6.00
(PtO$_2$H$_2$)$_{ads}$	2.024; 2.024; 2.063; 2.063	0.75	7.95
(PtO$_2$)$_{ads}$	1.843; 1.856; 2.101; 2.169	1.07	8.82
(Pt)$_{subCe}$	2.101; 2.159; 2.098; 2.164; 2.098; 2.175	1.35	10.60
(Pt)$_{subO}$	3.290	-0.86	4.11

Compared to the adsorption of CO on (Pt)$_{ads}$, a smaller adsorption energy (2.62 eV) was found for CO bound to (PtOH)$_{ads}$ species. This is due to the lower charge density of Pt in the (PtOH)$_{ads}$ configuration (Bader charge of 0.38 |e|), giving rise to a reducing effect of "π-back donation" from electrons in the 4d orbital of Pt to the antibonding $2\pi^{\star}$ orbital of the CO molecule. Therefore, the CO bond length (1.160 Å) is shorter than that of CO (1.169 Å) on (Pt)$_{ads}$ species, resulting in a stretching frequency of CO (2077 cm^{-1}) on (PtOH)$_{ads}$ that is 30 cm^{-1} larger than that on (Pt)$_{ads}$ (2047 cm^{-1}), as shown in Table 2. In addition, the smaller adsorption energy of CO on (PtOH)$_{ads}$ is evidenced by a larger C-Pt distance (1.837 Å) compared to that of CO on (Pt)$_{ads}$ (1.837 Å), Table 2 and Figure 3c.

A similar observation was found for CO bound to (PtO)$_{ads}$ with an adsorption energy of 2.63 eV. This is due to the similar charge density of Pt in the (PtOH)$_{ads}$ (Bader charge of 0.75 |e|) and (PtO)$_{ads}$ (Bader charge of 0.74 |e|) species. Furthermore, the CO bond length (1.160 Å) and C-Pt distance (1.840 Å) are also similar to those of CO on (PtOH)$_{ads}$ species (Table 2 and Figure 3d). This observation indicates that the two structures could have the same population on the CeO$_2$(111) surface.

A significant difference in adsorption energy was observed for CO on (PtO$_2$H$_2$)$_{ads}$ with a physisorption energy of 0.38 eV. This is similar to CO bound to the Ce(IV) site on the pristine material however, the vibrational stretching of CO is redshifted by 13 cm^{-1}, while a blueshift of the stretching frequency by +25 cm^{-1} was found for CO on the pristine material (Ta-
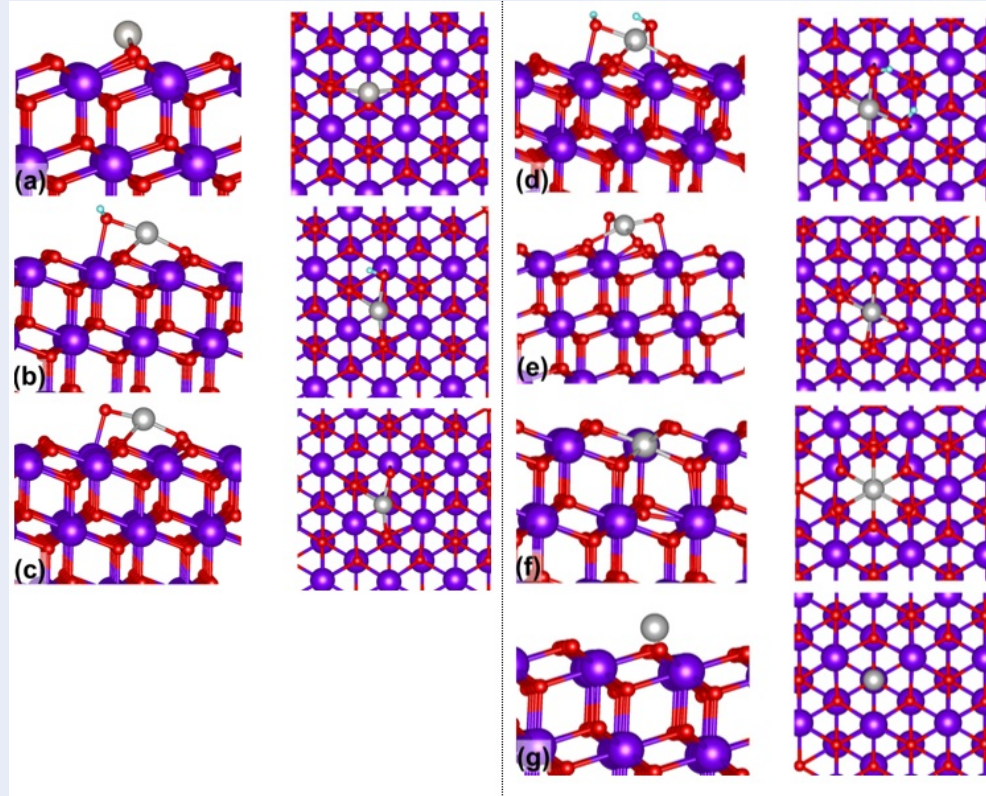
Figure 2: Side view (left) and top view (right) of a single Pt atom species on the CeO_2(111) surface. (a) $(Pt)_{ads}$, (b) $(PtOH)_{ads}$, (c) $(PtO)_{ads}$, (d) $(PtO_2H_2)_{ads}$, (e) $(PtO_2)_{ads}$, (f) $(Pt)_{subCe}$, (g) $(Pt)_{subO}$. O, Ce and Pt are red, purple and gray spheres, respectively.

ble 2). This is demonstrated further by the larger CO bond length (1.150 Å vs. 1.142 Å) and smaller C-Pt distance (1.875 Å vs. 2.820 Å), Table 2 and Figure 3e. Once the condensation process occurs, forming a H_2 molecule and leaving $(PtO_2)_{ads}$ species on the CeO_2(111) surface, CO was strongly bound to these $(PtO_2)_{ads}$ species with an adsorption energy of 1.37 eV, although the CO bond length (1.150 Å) and C-Pt distance (1.864 Å) are similar to those of CO on $(PtO_2H_2)_{ads}$.

For CO bound to (Pt_{subCe}) structures, a weak adsorption energy of 0.18 eV was observed, indicating that this CO complex could not be observed from the experiment existing in the literature [10,11,30,35] at room temperature. The physisorption of CO on this site is demonstrated by a large C-Pt distance of 3.43 Å and the small blueshift of the CO frequency (+9 cm^{-1}) with respect to the free CO molecule (Table 3 and Figure 3g). In contrast, CO is strongly bound to the (Pt_{subO}) structure with an adsorption energy of 1.12 eV. This is due to a larger charge density on the Pt center (Bader charge of -0.86 |e|) transferring to CO, re-

sulting in a prolonged CO bond length compared to that of CO in the gas phase (1.162 Å vs. 1.144 Å) (Table 3 and Figure 3h). As a consequence, the CO frequency is largely redshifted by -80 cm^{-1} compared to free CO.

CO adsorption on supported metallic Pt₃ clusters

For comparison to those of single Pt atom structures, the Pt_3 cluster deposited on the CeO_2(111) surface was adopted as a metallic model. The optimized structure of the Pt_3/CeO_2(111) surface is shown in Figure 4a, in which two bottom Pt atoms bound to surface O atoms with a distance of 1.93 Å and the third Pt atom is on the top forming a triangular Pt_3 cluster on the CeO_2(111) surface. The metallic properties of the Pt_3 cluster on the CeO_2(111) surface were confirmed by the Bader charge of 0.06 |e|. Furthermore, the interaction between Pt-Pt atoms in the Pt_3 cluster is also strong, with cohesive energies of 7.5 eV, but less than the interaction between a single Pt atom and the CeO_2(111) surface in the $(PtO_2)_{ads}$ species (8.82
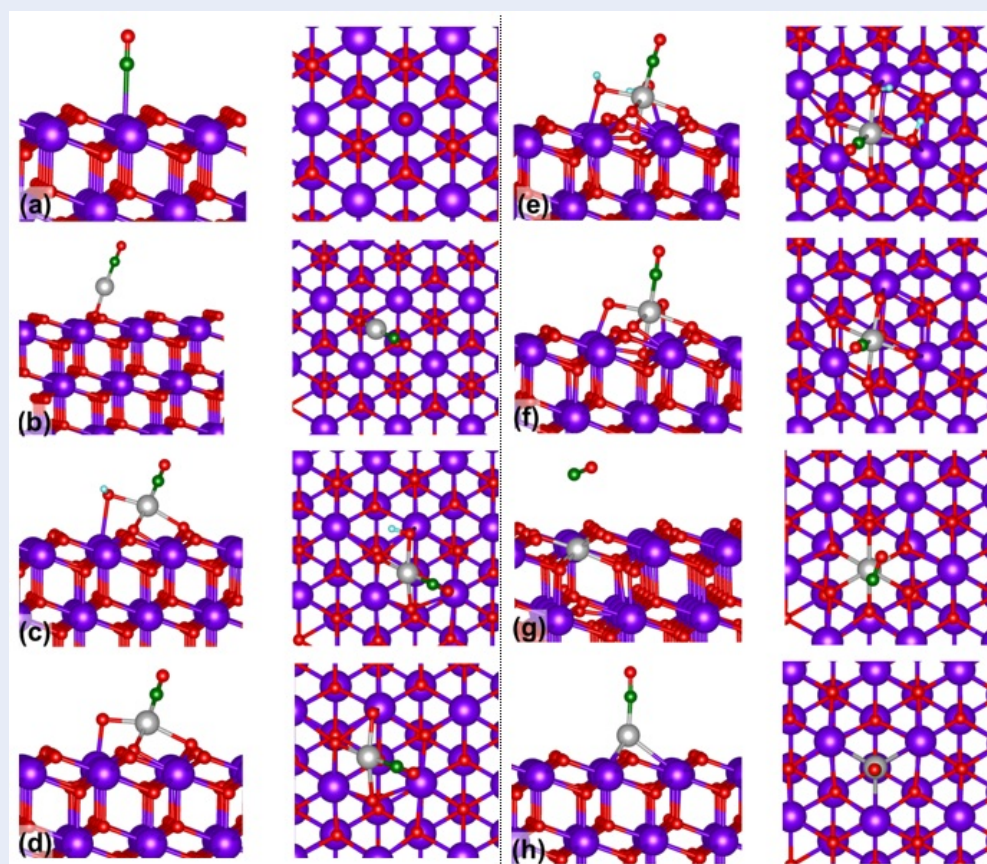
Figure 3: Side view (left) and top view (right) of CO adsorption on pristine and on single Pt atom species on CeO$_2$(111) surface. (a) Pristine CeO$_2$(111), (b) (Pt)$_{ads}$, (c) (PtOH)$_{ads}$, (d) (PtO)$_{ads}$, (e) (PtO$_2$H$_2$)$_{ads}$, (f) (PtO$_2$)$_{ads}$, (g) (Pt)$_{subCe}$, (h) (Pt)$_{subO}$. O, Ce,Pt and C are red, purple, gray and green spheres, respectively.

eV), Table 1. This implies that isolated Pt atoms in (PtO$_2$)$_{ads}$ are stable against the agglomeration of Pt. To probe the electronic properties of the supported Pt$_3$ cluster, all possible CO adsorption configurations on the Pt$_3$ cluster were considered, including Pt top, bridge and Pt interface sites (Figure 4). In either structure, CO is strongly bound to the supported Pt$_3$ cluster with similar adsorption energies in the range from 2.38 to 2.49 eV (Table 2). These results are in line with previous studies of CO adsorption on Pt$_3$/TiO$_2$(101) surfaces.[24] The strong binding of CO on the Pt$_3$ cluster is related to a large charge transfer from Pt$_3$ to CO, which prolonged the CO bond length in the range of 1.167- 1.191 Å. As a result, the large redshift of CO frequencies (-109, -115 and -270 cm^{-1} for CO on Pt top, bridge and Pt interface sites, respectively, Table 2). These observations are in good agreement with the experiment in reference[10]. This obviously indicates that the difference in electronic structure of single Pt atoms and their metallic counterparts can be clearly distinguished.

DISCUSSION

The nature of the high stability of single Pt atoms on the ceria surface has been theoretically studied on the basis of metal-support interactions between Pt atoms and the ceria surface, and they pointed out that the high thermal stability of the single Pt atoms on the ceria substrate is due to Pt atoms substitutional to Ce cations[35,36] or located at step edges.[37] In these defect sites, Pt is bound strongly with lattice O atoms forming a planar structure, resulting in the high thermal stability of single Pt atoms, which was experimentally demonstrated above 700 K.[37] Furthermore, such systems were found to have high selectivity for CO oxidation reactions via the Mars-van Krevelen mechanism. This is due to the active center of single Pt atoms, which can act as both an oxidant agent and reductive agent. Different from the previous theoretical studies mentioned above, here, to gain insight into the electronic and geometrical structure of a single Pt atom anchored on the CeO$_2$(111) surface, we

Table 2: CO adsorption site, CO adsorption energy, E_{ads} (eV), C-O bond length, R_{CO} (Å), C-M (M=Pt,Ce) distance, R_{CM} (Å), Bader charge of Pt (before) after CO adsorption, Q(Pt) (|e|), harmonic CO stretching frequency, ω_e (cm^{-1}) and frequency shift with respect to the gas-phase, $\triangle\omega_e$ (cm^{-1}) for CO adsorption on various single Pt atom species on CeO$_2$ (111) surfaces.

System	CO site	E_{ads} (eV)	R_{CO} (Å)	R_{CM} (Å)	Q(Pt) (|e|)	ω_e (cm^{-1})	$\triangle\omega_e$ (cm^{-1})
CeO$_2$(111)	Ce^{IV}	0.31	1.142	2.820	-	2168	25
(Pt)$_{ads}$	Pt^0	3.52	1.169	1.812	(0.04) 0.07	2047	-96
(PtOH)$_{ads}$	Pt^I	2.62	1.160	1.837	(0.38) 0.75	2077	-66
(PtO)$_{ads}$	Pt^I	2.63	1.160	1.840	(0.57) 0.74	2073	-70
(PtO$_2$H$_2$)$_{ads}$	Pt^{II}	0.38	1.150	1.875	(0.75) 1.29	2130	-13
(PtO$_2$)	Pt^{II}	1.37	1.150	1.864	(1.07) 1.25	2109	-24
(Pt)$_{subCe}$	Pt^{IV}	0.09	1.142	3.430	(1.35) 1.35	2147	+4
(Pt)$_{subO}$	Pt-^{II}	1.12	1.162	1.850	(-0.86) -0.37	2063	-80
Pt$_3$	Pt^0-top	2.46	1.166	1.834	(0.06) 0.06	2034	-109
Pt$_3$	Pt^0-bridge	2.49	1.191	1.938;1.947	(0.06) 0.12	1873	-270
Pt$_3$	Pt^0-interface	2.38	1.167	1.827	(0.06) 0.08	2028	-115
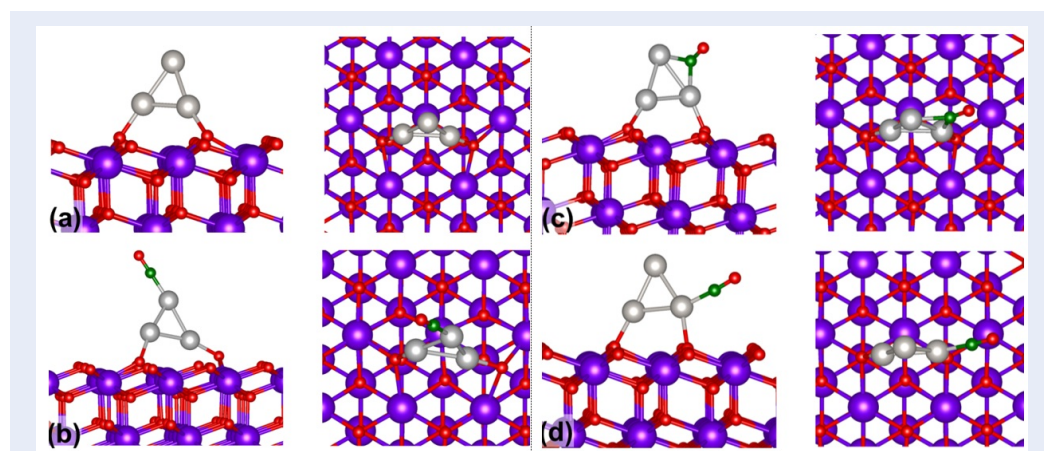
Figure 4: Side view (left) and top view (right) of the Pt$_3$ cluster and CO adsorption on Pt$_3$ adsorbed on the CeO$_2$(111) surface. (a) Pt$_3$, (b) CO at Pt top, (c) CO at bridge and (d) CO at Pt interface sites. O, Ce, Pt and C are red, purple, gray and green spheres, respectively.

mainly focus on the vibrational frequencies of CO adsorption on single Pt atom structures and compare them to experimental results existing from the literature.[10–12,30,38] There is a consistency from various experimental studies in the literature that the stretching frequencies of CO on single Pt atom species dispersed on CeO$_2$(111) surface are in the range from 2092-2102 cm^{-1},[10–12,30,38] which is completely different from those of CO on Pt metallic clusters[10] and

on bare CeO$_2$(111) surface (2159-2168 cm^{-1}).[10,30] Therefore, we can compare our results with these experimental results existing from the literature and provide in detail the electronic structures of single Pt atoms deposited on the real CeO$_2$ catalyst.

It is clear from the results in Table 2 that the stretching frequency of CO adsorbed on the pristine CeO$_2$(111) surface (2168 cm^{-1}) is blueshifted by 25 cm^{-1} and in excellent agreement with that observed from ex-

perimental studies in references [10,30]. Different from CO on the bare $CeO_2(111)$ surface, a large redshift of CO frequencies with respect to free CO molecules was found for CO adsorbed on $(Pt)_{ads}$, $(PtOH)_{ads}$, $(PtO)_{ads}$, and $(Pt)_{subO}$ by -96 cm^{-1}, -66 cm^{-1}, -70 cm^{-1} and -80 cm^{-1}, respectively. This is much far from the experimental observation, with a redshift of CO frequencies in the range from -51 cm^{-1} to -41 cm^{-1}. [10–12,30,38] This allows us to rule out these structures as single Pt atom structures, which were experimentally found on the $CeO_2(111)$ surface in the references [10–12,30,38].

For CO adsorption on $(PtO_2H_2)_{ads}$ and $(Pt)_{subCe}$, the very weak adsorption energy, which cannot form at experimental temperatures above room temperature, as mentioned in the literature [10,11,30], and the blueshift of adsorbed CO also allow us to exclude these structures existing as single atom species on the $CeO_2(111)$ surface.

Only in the case of CO on $(PtO_2)_{ads}$ was the stretching frequency of CO (2109 cm^{-1}) in good agreement with experimental observations (2190-2102 cm^{-1}) in the literature [10–12,30]. Furthermore, the Pt center coordinated with four O neighboring atoms that were also in line with experiments in the literature. [10,12] Therefore, this $(PtO_2)_{ads}$ configuration is a good presentation for the activity and high stability of a single Pt atom on the $CeO_2(111)$ surface.

It is also obvious that the frequencies (from 1873 cm^{-1} to 2034 cm^{-1}) of CO adsorbed on different sites of the Pt_3 cluster representative of metallic Pt on $CeO_2(111)$ were completely different from those on single Pt atoms and agree well with experimental data in references [10,30]. Therefore, these results can be used to differentiate with those of single Pt atom species.

CONCLUSIONS

The geometrical and electronic structure of a single Pt atom was investigated by means of the DFT+U method with dispersion corrections. Several structures of a single Pt atom have been considered, including $(Pt)_{ads}$, $(PtOH)_{ads}$, $(PtO)_{ads}$, $(PtO_2H_2)_{ads}$, $(PtO_2)_{ads}$, and $(Pt)_{subCe}$ và $(Pt)_{subO}$. Furthermore, the supported Pt_3 cluster for the metallic model was considered for further comparison. To probe the differences in the electronic structure of single Pt atom species and Pt_3 clusters, the adsorption energies and stretching frequencies of CO adsorption on these configurations were evaluated. Based on these results and compared to experiments, we found that the high activity and high stability of a single Pt atom anchored on the $CeO_2(111)$ surface is formed by the interaction between the Pt atom and two extra O atoms

$(PtO_2)_{ads}$, resulting from the condensation process of Pt with two OH groups. Our observation is different from previous theoretical studies, in which they pointed out that the high thermal stability of single Pt atoms anchored on the $CeO_2(111)$ surface is due to the substitution of Pt into Ce sites [35,36] or located at step edges. [37] Therefore, our theoretical results provide another insight into single Pt atom structures on the $CeO_2(111)$ surface, and this study provides useful information for experiments in synthesis and important applications, especially CO oxidation [6,38] and water-gas shift reactions. [39]

ABREVIATIONS

DFT: density functional theory
VASP: Vienna Ab initio Simulation Package

COMPETING INTERESTS

The authors declare that there are no conflicts of interest regarding the publication of this paper.

ACKNOWLEDGMENTS

REFERENCES

1. Kurzman JA, Misch LM, Seshadri R. Chemistry of precious metal oxides relevant to heterogeneous catalysis. Dalton Trans. 2013 Oct 1;42(41):14653-67;PMID: 24008693. Available from: https://doi.org/10.1039/c3dt51818c.

2. Antoni M, Muench F, Kunz U, Brötz J, Donner W, Ensinger W. Electrocatalytic applications of platinum-decorated TiO2 nanotubes prepared by a fully wet-chemical synthesis. J Mater Sci. 2017 Jul 1;52(13):7754-67;Available from: https://doi.org/10.1007/s10853-017-1035-4.

3. Sun R, Liao Y, Bai S-T, Zheng M, Zhou C, Zhang T, et al. Heterogeneous catalysts for CO2 hydrogenation to formic acid/formate: from nanoscale to single atom. Energy Environ Sci. 2021 Mar 23;14(3):1247-85;Available from: https://doi.org/10.1039/D0EE03575K.

4. Whang HS, Lim J, Choi MS, Lee J, Lee H. Heterogeneous catalysts for catalytic CO2 conversion into value-added chemicals. BMC Chemical Engineering. 2019 Mar 27;1(1):9;Available from: https://doi.org/10.1186/s42480-019-0007-7.

5. Liu L, Corma A. Metal Catalysts for Heterogeneous Catalysis: From Single Atoms to Nanoclusters and Nanoparticles. Chem Rev. 2018 May 23;118(10):4981-5079;PMID: 29658707. Available from: https://doi.org/10.1021/acs.chemrev.7b00776.

6. Qiao B, Wang A, Yang X, Allard LF, Jiang Z, Cui Y, et al. Single-atom catalysis of CO oxidation using Pt1/FeOx. Nature Chem. 2011 Aug;3(8):634-41;PMID: 21778984. Available from: https://doi.org/10.1038/nchem.1095.

7. Wang A, Li J, Zhang T. Heterogeneous single-atom catalysis. Nat Rev Chem. 2018 Jun;2(6):65-81;Available from: https://doi.org/10.1038/s41570-018-0010-1.

8. Xi J, Jung HS, Xu Y, Xiao F, Bae JW, Wang S. Synthesis Strategies, Catalytic Applications, and Performance Regulation of Single-Atom Catalysts. Advanced Functional Materials. 2021;31(12):2008318;Available from: https://doi.org/10.1002/adfm.202008318.

9. Fan J, Chen Y, Jiang X, Yao P, Jiao Y, Wang J, et al. A simple and effective method to synthesize Pt/CeO2 three-way catalysts with high activity and hydrothermal stability. Journal of Environmental Chemical Engineering. 2020 Oct 1;8(5):104236;Available from: https://doi.org/10.1016/j.jece.2020.104236.

10. Resasco J, DeRita L, Dai S, Chada JP, Xu M, Yan X, et al. Uniformity Is Key in Defining Structure-Function Relationships for Atomically Dispersed Metal Catalysts: The Case of Pt/CeO2. J Am Chem Soc. 2020 Jan 8;142(1):169-84;PMID: 31815460. Available from: https://doi.org/10.1021/jacs.9b09156.

11. Jones J, Xiong H, DeLaRiva AT, Peterson EJ, Pham H, Challa SR, et al. Thermally stable single-atom platinum-on-ceria catalysts via atom trapping. Science. 2016 Jul 8;353(6295):150-4;PMID: 27387946. Available from: https://doi.org/10.1126/science.aaf8800.

12. Kunwar D, Zhou S, DeLaRiva A, Peterson EJ, Xiong H, Pereira-Hernández XI, et al. Stabilizing High Metal Loadings of Thermally Stable Platinum Single Atoms on an Industrial Catalyst Support. ACS Catal. 2019 May 3;9(5):3978-90;Available from: https://doi.org/10.1021/acscatal.8b04885.

13. Kresse G, Furthmüller J. Efficiency of ab-initio total energy calculations for metals and semiconductors using a plane-wave basis set. Computational Materials Science [Internet]. 1996 Jul 1 [cited 2020 Jan 2];Available from: https://www.scienceopen.com/document?vid=cad1a83f-e3bd-4d52-8db1-25b5f8305d9e.

14. Perdew JP, Burke K, Ernzerhof M. Generalized Gradient Approximation Made Simple. Phys Rev Lett. 1996 Oct 28;77(18):3865-8;PMID: 10062328. Available from: https://doi.org/10.1103/PhysRevLett.77.3865.

15. Blöchl PE. Projector augmented-wave method. Phys Rev B. 1994 Dec 15;50(24):17953-79;PMID: 9976227. Available from: https://doi.org/10.1103/PhysRevB.50.17953.

16. Dudarev SL, Botton GA, Savrasov SY, Humphreys CJ, Sutton AP. Electron-energy-loss spectra and the structural stability of nickel oxide: An LSDA+U study. Phys Rev B. 1998 Jan 15;57(3):1505-9;Available from: https://doi.org/10.1103/PhysRevB.57.1505.

17. Anisimov VI, Zaanen J, Andersen OK. Band theory and Mott insulators: Hubbard U instead of Stoner I. Phys Rev B. 1991 Jul 15;44(3):943-54;PMID: 9999600. Available from: https://doi.org/10.1103/PhysRevB.44.943.

18. Huang M, Fabris S. CO Adsorption and Oxidation on Ceria Surfaces from DFT+U Calculations. J Phys Chem C. 2008 Jun 1;112(23):8643-8;Available from: https://doi.org/10.1021/jp709898r.

19. Kümmerle EA, Heger G. The Structures of C-Ce2O3+δ, Ce7O12, and Ce11O20. Journal of Solid State Chemistry. 1999 Nov 1;147(2):485-500;Available from: https://doi.org/10.1006/jssc.1999.8403.

20. Grimme S, Antony J, Ehrlich S, Krieg H. A consistent and accurate ab initio parametrization of density functional dispersion correction (DFT-D) for the 94 elements H-Pu. J Chem Phys. 2010 Apr 21;132(15):154104;PMID: 20423165. Available from: https://doi.org/10.1063/1.3382344.

21. Thang HV, Maleki F, Tosoni S, Pacchioni G. Vibrational Properties of CO Adsorbed on Au Single Atom Catalysts on TiO2(101), ZrO2(101), CeO2(111), and LaFeO3(001) Surfaces: A DFT Study. Top Catal [Internet]. 2021 Dec 14 [cited 2022 Jan 20];Available from: https://doi.org/10.1007/s11244-021-01514-0.

22. Yang ZX, Ma DW, Yu XH, Hermansson K. The main factors influencing the O vacancy formation on the Ir doped ceria surface: A DFT+U study. Eur Phys J B. 2010 Oct 1;77(3):373-80;Available from: https://doi.org/10.1140/epjb/e2010-00295-x.

23. Tovt A, Bagolini L, Dvořák F, Tran N-D, Vorokhta M, Beranová K, et al. Ultimate dispersion of metallic and ionic platinum on ceria. J Mater Chem A. 2019 May 28;7(21):13019-28;Available from: https://doi.org/10.1039/C9TA00823C.

24. Thang HV, Pacchioni G, DeRita L, Christopher P. Nature of stable single atom Pt catalysts dispersed on anatase TiO2. Journal of Catalysis. 2018 Nov 1;367:104-14;Available from: https://doi.org/10.1016/j.jcat.2018.08.025.

25. Thang HV, Pacchioni G. Nature of Atomically Dispersed Ru on Anatase TiO2: Revisiting Old Data Based on DFT Calculations. J Phys Chem C. 2019 Mar 28;123(12):7271-82;Available from: https://doi.org/10.1021/acs.jpcc.9b00977.

26. DeRita L, Resasco J, Dai S, Boubnov A, Thang HV, Hoffman AS, et al. Structural evolution of atomically dispersed Pt catalysts dictates reactivity. Nat Mater. 2019 Jul;18(7):746-51;PMID: 31011216. Available from: https://doi.org/10.1038/s41563-019-0349-9.

27. Mina-Camilde N, Manzanares I. C, Caballero JF. Molecular Constants of Carbon Monoxide at v = 0, 1, 2, and 3: A Vibrational Spectroscopy Experiment in Physical Chemistry. J Chem Educ. 1996 Aug 1;73(8):804;Available from: https://doi.org/10.1021/ed073p804.

28. Yu M, Trinkle DR. Accurate and efficient algorithm for Bader charge integration. J Chem Phys. 2011 Feb 14;134(6):064111;PMID: 21322665. Available from: https://doi.org/10.1063/1.3553716.

29. Jan A, Shin J, Ahn J, Yang S, Yoon KJ, Son J-W, et al. Promotion of Pt/CeO2 catalyst by hydrogen treatment for low-temperature CO oxidation. RSC Adv. 2019 Aug 23;9(46):27002-12;Available from: https://doi.org/10.1039/C9RA05965B.

30. Maurer F, Jelic J, Wang J, Gänzler A, Dolcet P, Wöll C, et al. Tracking the formation, fate and consequence for catalytic activity of Pt single sites on CeO2. Nat Catal. 2020 Oct;3(10):824-33;Available from: https://doi.org/10.1038/s41929-020-00508-7.

31. Han Z-K, Zhang L, Liu M, Ganduglia-Pirovano MV, Gao Y. The Structure of Oxygen Vacancies in the Near-Surface of Reduced CeO2 (111) Under Strain. Frontiers in Chemistry [Internet]. 2019 [cited 2022 Jan 15];7;PMID: 31275923. Available from: https://doi.org/10.3389/fchem.2019.00436.

32. Tosoni S, Li C, Schlexer P, Pacchioni G. CO Adsorption on Graphite-like ZnO Bilayers Supported on Cu(111), Ag(111), and Au(111) Surfaces. J Phys Chem C. 2017 Dec 14;121(49):27453-61;Available from: https://doi.org/10.1021/acs.jpcc.7b08781.

33. Pacchioni G, Cogliandro G, Bagus PS. Molecular orbital cluster model study of bonding and vibrations of CO adsorbed on MgO surface. International Journal of Quantum Chemistry. 1992;42(5):1115-39;Available from: https://doi.org/10.1002/qua.560420504.

34. Velasquez J, Duncan MA. IR photodissociation spectroscopy of gas phase Pt+(CO)n (n=4-6). Chemical Physics Letters. 2008 Aug 8;461(1):28-32;Available from: https://doi.org/10.1016/j.cplett.2008.06.084.

35. Qin Y-Y, Su Y-Q. A DFT Study on Heterogeneous Pt/CeO2(110) Single Atom Catalysts for CO Oxidation. ChemCatChem. 2021;13(17):3857-63;Available from: https://doi.org/10.1002/cctc.202100643.

36. Tang Y, Wang Y-G, Li J. Theoretical Investigations of Pt1@CeO2 Single-Atom Catalyst for CO Oxidation. J Phys Chem C. 2017 Jun 1;121(21):11281-9;Available from: https://doi.org/10.1021/acs.jpcc.7b00313.

37. Dvořák F, Farnesi Camellone M, Tovt A, Tran N-D, Negreiros FR, Vorokhta M, et al. Creating single-atom Pt-ceria catalysts by surface step decoration. Nat Commun. 2016 Feb 24;7(1):10801;Available from: https://doi.org/10.1038/ncomms10801.

38. Nie L, Mei D, Xiong H, Peng B, Ren Z, Hernandez XIP, et al. Activation of surface lattice oxygen in single-atom Pt/CeO2 for low-temperature CO oxidation. Science [Internet]. 2017 Dec 15 [cited 2022 Jan 16];Available from: https://www.science.org/doi/abs/10.1126/science.aao2109.

39. Li Y, Kottwitz M, Vincent JL, Enright MJ, Liu Z, Zhang L, et al. Dynamic structure of active sites in ceria-supported Pt catalysts for the water gas shift reaction. Nat Commun. 2021 Feb 10;12(1):914;Available from: https://doi.org/10.1038/s41467-021-21132-4.